JOURNAL OF VIROLOGY, Dec. 2008, p. 12555–12564 Vol. 82, No. 24
0022-538X/08/$08.00+0 doi:10.1128/JVI.01238-08

Characterization of White Spot Syndrome Virus Envelope Protein VP51A and Its Interaction with Viral Tegument Protein VP26▽

Yun-Shiang Chang,[1]* Wang-Jing Liu,[2] Tsung-Lu Chou,[1] Yuan-Ting Lee,[1] Tai-Lin Lee,[1] Wei-Tung Huang,[1] Guang-Hsiung Kou,[2] and Chu-Fang Lo[2]*

Department of Molecular Biotechnology, Da-Yeh University, Changhua, Taiwan,[1] and Institute of Zoology, National Taiwan University, Taipei, Taiwan[2]

Received 14 June 2008/Accepted 17 September 2008

In this study, we characterize a novel white spot syndrome virus (WSSV) structural protein, VP51A (WSSV-TW open reading frame 294), identified from a previous mass spectrometry study. Temporal-transcription analysis showed that *vp51A* is expressed in the late stage of WSSV infection. Gene structure analysis showed that the transcription initiation site of *vp51A* was 135 bp upstream of the translation start codon. The poly(A) addition signal overlapped with the translation stop codon, TAA, and the poly(A) tail was 23 bp downstream of the TAA. Western blot analysis of viral protein fractions and immunoelectron microscopy both suggested that VP51A is a viral envelope protein. Western blotting of the total proteins extracted from WSSV virions detected a band that was close to the predicted 51-kDa mass, but the strongest signal was around 72 kDa. We concluded that this 72-kDa band was in fact the full-length VP51A protein. Membrane topology assays demonstrated that the VP51A 72-kDa protein is a type II transmembrane protein with a highly hydrophobic transmembrane domain on its N terminus and a C terminus that is exposed on the surface of the virion. Coimmunoprecipitation, colocalization, and yeast two-hybrid assays revealed that VP51A associated directly with VP26 and indirectly with VP28, with VP26 acting as a linker protein in the formation of a VP51A-VP26-VP28 complex.

Viral structural proteins, especially the envelope proteins, are important, not only because they are involved in virion morphogenesis, but also because they are the first molecules to interact with the host. The structural proteins often play vital roles in cell targeting, virus entry, assembly, and budding (1, 2, 21, 22, 24), as well as triggering host antiviral defenses (26). In the case of white spot syndrome virus (WSSV) (genus *Whispovirus*, family *Nimaviridae*) (37), a double-stranded DNA virus that has caused severe mortality and huge economic losses to the shrimp farming industry globally for more than a decade (5, 19), proteomic methods have helped to identify a total of 58 structural proteins, over 30 of which are currently recognized as envelope proteins (13, 31, 44, 47). Some of the WSSV envelope proteins involved in shrimp infection have been identified (12, 14, 34, 36, 41, 43), and these envelope and other WSSV structural proteins have been used in various studies, including RNA interference-based gene knockdown to silence viral structural-protein gene expression (8, 27, 45), DNA and protein vaccination to elevate host immunity (25, 29, 36, 39), and antibody neutralization techniques that neutralize the virus by preventing envelope proteins from interacting with host cell receptors (12, 34, 41, 43).

In the present paper, we characterize and investigate the functionality of a WSSV structural protein that was first reported by Tsai et al. (32). This protein, designated VP51A, corresponds to open reading frame 294 of the WSSV-TW isolate, and its gene encodes a polypeptide of 486 amino acids (aa) with a theoretical mass of 51 kDa. A method was recently established to assign the WSSV structural proteins to one of three morphologically distinct substructures in the virion: the nucleocapsid, the intermediate tegument layer that surrounds the nucleocapsid, and the outer viral envelope (31). We use the same method here to show that VP51A is an envelope protein, and we support this conclusion with an in vivo immunogold assay. Some WSSV structural proteins are known to interact with other structural proteins. For example, VP28 interacts with VP24 and VP26 (43, 44), and VP24 interacts with another WSSV envelope protein, WSV010 (3). Identification of these relationships among structural proteins is a significant step toward understanding the function of each protein and is potentially helpful in developing effective anti-WSSV strategies. We show here that VP51A forms a complex with two other major WSSV structural proteins, VP26 and VP28.

MATERIALS AND METHODS

Virus. The WSSV-TW strain was isolated from a batch of WSSV-infected *Penaeus monodon* shrimp collected in Taiwan in 1994 (18, 38), and it was used as the template for amplification of the *vp51A*, *vp26*, and *vp28* coding regions in all of the following experiments.

Temporal-transcription analysis of *vp51A* by RT-PCR. Adult *P. monodon* shrimp (mean weight, ~20 g) were experimentally infected with WSSV by injection and subsequently collected at 0 (i.e., immediately before infection), 2, 4, 6, 12, 24, 36, 48, and 60 h postinfection (p.i.) according to a procedure described by Tsai et al. (33). Total RNAs were isolated from the gills of the sampled shrimp by using Trizol reagent (Invitrogen Corp.) according to the manufacturer's instructions. The isolated RNAs were treated with DNase I (Roche) at 37°C for 1 h and then recovered by phenol-chloroform-isoamyl alcohol extraction and ethanol precipitation. The RNAs were reverse transcribed with SuperScript II re-

* Corresponding author. Mailing address for Chu-Fang Lo: Institute of Zoology, National Taiwan University, Taipei 106, Taiwan. Phone: 886-2-33662453. Fax: 886-2-23638179. E-mail: gracelow@ntu.edu.tw. Mailing address for Yun-Shiang Chang: Department of Molecular Biotechnology, Da-Yeh University, Changhua 515, Taiwan. Phone: 886-4-8511888, ext. 4265. Fax: 886-4-8511326. E-mail: yschang@mail.dyu.edu.tw.

▽ Published ahead of print on 1 October 2008.

TABLE 1. Primer sequences for 5′/3′ RACE and RT-PCR

Gene	Primer	Sequence (5′–3′)	Usage
vp51A	WSSV294-F-122	GGAAGAGATATCGTACCAGTGAG	*vp51A* RT-PCR
	WSSV294-R-632	CTTGGTTTTCCTTGTAGAGTGTC	
ie1	ie1-F	GACTCTACAAATCTCTTTGCCA	*ie1* RT-PCR
	ie1-R	CTACCTTTGCACCAATTGCTAG	
dnapol	dnapol-F	TGGGAAGAAAGATGCGAGAG	*dnapol* RT-PCR
	dnapol-R	CCCTCCGAACAACATCTCAG	
vp28	vp28-F	CTGCTGTGATTGCTGTATTT	*vp28* RT-PCR
	vp28-R	CAGTGCCAGAGTAGGTGAC	
actin 2	P1882-actin F1	CCGTCATCAGGGTGTGATGGT	*actin* RT-PCR
	P1883-actin R	CCACGCTCAGTCATGATCTTCA	
vp51A	*vp51A* SP1	GTAGGCTCAAAATCGTCTGTGTC	*vp51A* 5′ RACE
vp51A	*vp51A* SP2	GAACCATTTCCATTTGTTCCAC	*vp51A* 5′ RACE
vp51A	*vp51A* SP3	TTGTTCCAGTTCCTCCGTCTAT	*vp51A* 5′ RACE
vp51A	*vp51A* SP4	TTGTGGCCAATAAGAATGACAC	*vp51A* 3′ RACE

verse transcriptase (RT) (Invitrogen Corp.) and an oligo(dT) anchor primer (Roche). The first-strand cDNA products were subjected to PCR with the *vp51A* primers WSSV294-F-122 and WSSV294-R-632 (Table 1). For comparison, the WSSV *ie1* (an immediate-early gene), *dnapol* (a DNA polymerase gene), and *vp28* (an envelope protein gene) gene fragments were also amplified from the same templates using the primer pairs ie1-F/ie1-R, dnapol-F/dnapol-R, and vp28-F/vp28-R, respectively (Table 1). An *actin 2* primer pair, P1882-actin F1 and P1883-actin R1, designed by Leu et al. (11) and based on *P. monodon actin 2* (AF100987), was used as an internal control for RNA quantity and amplification efficiency. The primer sequences are listed in Table 1.

Mapping the 5′ and 3′ termini of *vp51A* transcripts. The 5′ and 3′ regions of the *vp51A* transcripts were obtained by 5′/3′ rapid amplification of cDNA ends (RACE) (6) using a commercial 5′/3′ RACE kit (Roche) with an avian myeloblatosis virus RT. The RNA samples used for 5′/3′ RACE analysis were isolated from the gills of WSSV-infected *P. monodon* at 36 h p.i. and treated with DNase I as described above. The appropriate gene-specific primers used for 5′/3′ RACE are listed in Table 1. The final amplification products were cloned into the pGEM-T Easy vector (Promega) and sequenced. The sequences of the inserts were compared with the WSSV genomic-DNA sequences.

Expression, purification of recombinant VP51A proteins, and antibody production. PCR fragments representing three different coding regions of *vp51A* were amplified using the primer sets listed in Table 2, digested with restriction enzymes, and cloned into pET-28b(+) (Novagen). The resulting plasmids, pET-28b/VP51A$_{139\text{-}250}$, pET-28b/VP51A$_{251\text{-}486}$, and pET-28b/VP51A$_{51\text{-}486}$ (containing the VP51A aa residues 139 to 250, 251 to 486, and 51 to 486, respectively), were transformed into BL21 Codon Plus *Escherichia coli* cells (Stratagene) and used for protein production. The transformed cells were grown overnight at 37°C in Luria-Bertani medium supplemented with 50 μg/ml kanamycin. The cells were then inoculated into fresh medium at a ratio of 1:50 and grown at 37°C for 1.5 to 2 h. Expression was induced by the addition of 1 mM IPTG (isopropyl-β-D-thiogalactopyranoside), and incubation was continued for another 1.5 to 3 h. The induced bacteria were spun down at 4°C, suspended in ice-cold 1× phosphate-buffered saline (PBS) containing 10% glycerol and a protease inhibitor cocktail tablet (Roche), and sonicated for 3 min on ice. The insoluble debris was collected by centrifugation, suspended in 1× PBS containing 1.5% sodium lauryl sarcosine, and solubilized by shaking at room temperature for 1 h. The supernatant was clarified by centrifugation and mixed with Ni-nitrilotriacetic acid-agarose beads (Qiagen) on a rotating wheel at 4°C for 16 h. The beads were then washed several times with ice-cold wash buffer (1 M NaCl, 10 mM Tris-HCl, pH 7.5) to remove unbound material. The fusion proteins were eluted directly from the beads with sodium dodecyl sulfate (SDS) sample buffer and were then subjected to SDS-polyacrylamide gel electrophoresis (PAGE) analysis. For polyclonal-antibody production from the VP51A midsequence (aa 139 to 250) and C-terminal (aa 251 to 486) fragments, the protein bands containing the fusion proteins were sliced from the gel, minced, mixed with Freund's adjuvant, and inoculated into rabbits.

TABLE 2. Primer sequences used for the construction of various expression plasmids

Construct	Primer[a]	Sequence (5′–3′)[b]	Tag
pET-28b/VP51A$_{139\text{-}250}$	F	CGCGGATCCGGATACAGACACAGACGATTTTGAG	His
	R	CCCAAGCTTTAATATTGTTTGTGCAATTTC	
pET-28b/VP51A$_{251\text{-}486}$	F	GGCGAGCTCCAGTCAACTAAGAGAAAAACAC	His
	R	CCCAAGCTTTGGCTGGACAATAAATTTTTG	
pET-28b/VP51A$_{51\text{-}486}$	F	CGGGATCCTGACGGCATAGACGGAGGAACT	His
	R	CCCAAGCTTTGGCTGGACAATAAATTTTTG	
pcDNA3/VP51A	F	CCCAAGCTTGAAAAAATGTTCGTCATAAGC	None
	R	CGCGGATCCTTATTGGCTGGACAATAAATTTTT	
pDHsp/VP51A-FLAG-His	F	CCCAAGCTTGAAAAAATGTTCGTCATAAGC	Flag/V5
pDHsp/VP51A-V5-His	R	TCCCCGCGGTTGGCTGGACAATAAATTTTTG	
pDHsp/VP26-FLAG-His	F	CCCAAGCTTAGAAAAATGGAATTTGGCAAC	Flag/V5
pDHsp/VP26-V5-His	R	TCCCCGCGGCTTCTTCTTGATTTCGTCCTTG	
pDHsp/VP28-V5-His	F	CCCAAGCTTCTCGTCATGGATCTTTCTTTC	V5
	R	TCCCCGCGGCTCGGTCTCAGTGCCAGAGTAG	
pGBK-VP51A	F	TCCCCCGGGAATGTTCGTCATAAGCATAGC	c-Myc
	R	CGGGATCCTTATTGGCTGGACAATAAATT	
pGAD-VP26	F	CGGAATTCATGGAATTTGGCAACCTAAC	HA[c]
	R	CCGCTCGAGGCTTCTTCTTGATTTCGTCCT	
pGAD-VP28	F	CGGAATTCATGGATCTTTCTTTCACTCTTT	HA
	R	CCGCTCGAGGCTCGGTCTCAGTGCCAGAGTA	

[a] F, forward; R, reverse.
[b] The restriction enzyme cutting sites are underlined.
[c] HA, hemagglutinin.

Fractionation of virion proteins by detergent treatment at different NaCl concentrations. Adult crayfish, *Procambarus clarkia*, were challenged with WSSV, and the virions were purified from the hemolymph of the infected crayfish as described by Tsai et al. (32). The purified virus suspension was treated with 1% Triton X-100 in different concentrations (0, 0.1, 0.5, and 1 M) of NaCl solution, and the soluble and insoluble portions were then fractionated by centrifugation as described previously (31). The intact untreated virion suspension served as a control. The proteins in each of the eight resultant fractions and in the intact purified virion control were resolved by Western blot analysis using the anti-VP51A C-terminal-fragment antibody. The bound antibodies were then stripped out of the membrane, and the membrane was reprobed with antibodies to the WSSV envelope protein VP28, to the tegument protein VP26, and to the nucleocapsid protein VP51C (31, 40). An additional Western blot analysis was performed on the intact purified virion proteins using the anti-VP51A midsequence fragment antibody as the probe.

Western blot analysis. Protein samples were resolved by SDS-PAGE. After separation, the proteins were transferred to polyvinylidene difluoride membranes (MSI). The membranes were incubated in blocking buffer (5% skim milk in Tris-buffered saline [50 mM Tris, 500 mM NaCl, pH 7.5]) at 4°C overnight and then incubated with blocking buffer containing primary antibodies for 1 h at room temperature. Next, the membrane was washed three times with 0.5% Tween 20 in Tris-buffered saline and incubated with a horseradish peroxidase (HRP)-conjugated secondary antibody. After three more washes, the proteins were visualized by use of a chemiluminescence reagent (Perkin-Elmer, Inc.).

Localization of VP51A by immunoelectron microscopy (IEM). Following the method of Tsai et al. (31), aliquots (10 μl) of purified virion suspension were adsorbed to Formvar-supported, carbon-coated nickel grids (200 mesh) for 5 min at room temperature, and then the excess solution was removed. The grids were either prefixed for 5 min with 4% paraformaldehyde and 1% Triton X-100 simultaneously in 50 mM Tris buffer (to remove the virus envelope) or were left unfixed and were incubated with incubation buffer only (0.1% Aurion BSA-c, 15 mM NaN_3, 10 mM phosphate buffer, 150 mM NaCl, pH 7.4). Other grids were loaded with purified nucleocapsid samples (5-min absorption at room temperature) prepared by treating purified virions with detergent and NaCl, followed by centrifugal fractionation (31). These nucleocapsid grids were left unfixed. All grids were then blocked with blocking buffer (5% bovine serum albumin, 5% normal goat serum, 0.1% cold-water fish skin gelatin [Aurion], 10 mM phosphate buffer, 150 mM NaCl, pH 7.4) for 15 min and then incubated for 1 h at room temperature with VP51A C-terminal antibody diluted 1:50 in incubation buffer. As a control, an additional grid containing intact virions was incubated using a dilution of preimmune rabbit serum instead of the anti-VP51A C-terminal antibody. After several washes with incubation buffer, the grids were incubated for 1 h at room temperature with a goat anti-rabbit secondary antibody conjugated with 15-nm-diameter gold particles (1:40 dilution in incubation buffer). The grids were then washed extensively with incubation buffer, washed twice more with distilled water to remove excess salt, and stained with 2% phosphotungstic acid (pH 7.4) for 30 s. Specimens were examined with a transmission electron microscope (Jeol JEM1010).

Coupled in vitro transcription and translation. A full-length *vp51A* expression plasmid, pcDNA3/VP51A, was constructed by using PCR to clone the *vp51A* coding region into the commercial vector pcDNA3 (Invitrogen Corp.). The primers used for the PCR cloning are listed in Table 2. Coupled in vitro transcription-translation reactions were conducted in accordance with the manufacturer's protocol (TNT System; Promega). One microgram of plasmid pcDNA3/VP51A DNA and 1 μl of [^{35}S]methionine (1,000 Ci/mmol; 10 mCi/ml) were added to the TNT reaction mixture to make a total volume of 50 μl, and the reaction proceeded at 30°C for 90 min. An aliquot of the translation product (5 μl) was analyzed by 15% SDS-PAGE. After electrophoresis, the gel was fixed and exposed to Kodak Biomax MS film.

Computer analysis of the VP51A coding region. Based on the deduced amino acid sequence of VP51A, its hydropathic profile was predicted by a computer-assisted procedure that followed the methods of Kyte and Doolittle (10). Topology predictions were made using the TMHMM (9) program. Both of these programs are accessible on the World Wide Web (http://ca.expasy.org/tools/).

VP51A topology. To investigate the membrane topology of VP51A, the plasmid pDHsp/VP51A-V5-His was constructed by inserting the full-length WSSV *vp51A* gene into a V5-tagged vector containing the heat-inducible *Drosophila* heat shock protein 70 promoter (pDHsp/V5-His) (11) by PCR cloning using WSSV genomic DNA as the template. The primers used for this PCR are listed in Table 2. Using Cellfectin reagent (Invitrogen Corp.), this plasmid was transfected into Sf9 insect cells that had been seeded onto cover glasses placed in each well of a four-well microplate (1×10^5 cells/well) and grown in Sf-900 II serum-free medium (Invitrogen Corp.) overnight at 27°C. After transfection for 16 to 18 h, the cells were heat shocked in a 42°C water bath for 30 min and then returned to 27°C. At 6 h after heat induction, the monolayers were washed with PBS and the cells were fixed in paraformaldehyde (4% in PBS) for 10 min at 4°C. Some cells were then treated with 0.1% Triton X-100 in 4% paraformaldehyde/PBS solution for 3 min at 4°C, while other cells were left untreated. All the cells were then washed thoroughly two times with PBS. After being blocked in blocking buffer (5% bovine serum albumin and 2% normal goat serum in PBS) for 16 h at 4°C, the cells were treated with a 1,000× PBS-diluted polyclonal rabbit anti-V5 antibody (Sigma) (3 h at room temperature). Next, the cells were washed three times (10 min each time) with PBST (0.2% Tween 20 in PBS) and reacted with carboxymethylindocyanine (Cy3) dye-conjugated donkey anti-rabbit immunoglobulin G (IgG) antibody (1:1,000 in PBS; Jackson ImmunoResearch) for 2 h at room temperature. Counterstaining of the nucleus was performed with 4′-6′-diamidino-2-phenylindole dihydrochloride (DAPI) (Vector Laboratories). After being washed three times (10 min each time) with PBST, the cover glasses were wet mounted with antifade mounting medium (Fluka). During all of the above-mentioned procedures, the cells were kept in darkness. Fluorescence signals were examined using a confocal scanning laser microscope (Leica TCS SP5).

To investigate the topology of VP51A, VP28, and VP26 in the WSSV virion, we followed the method of Zhu and Yuan (48) and treated aliquots (5 μg of total protein) of purified virions with trypsin (5 μg/ml; Promega) in 100 μl of buffer (50 mM Tris-HCl [pH 7.5], 1 mM $CaCl_2$, 100 mM NaCl) at 37°C for 2 h. Trypsin digestion was terminated by adding phenylmethylsulfonyl fluoride to a final concentration of 0.5 mM and then adding 1/50 volume of protease inhibitor. In some samples, prior to trypsin digestion, Triton X-100 was added to a final concentration of 1% to dissolve the viral envelope and expose the internal structure to the protease. Samples were analyzed by Western blotting using antibodies to VP51A, to the envelope protein VP28, and to the tegument protein VP26.

Coimmunoprecipitation. Full-length WSSV *vp51A*, *vp26*, and *vp28* genes were inserted into V5- or FLAG-tagged vectors containing the heat-inducible *Drosophila* heat shock protein 70 promoter (pDHsp/V5-His and pDHsp/FLAG-His) (11) by PCR cloning using WSSV genomic DNA as the template. The primers used for PCR are listed in Table 2. For DNA transfection, Sf9 insect cells were seeded onto a six-well plate (8×10^5 cells/well) and grown overnight. Plasmids containing the appropriate genes (including the empty vector) were transfected into the Sf9 cells for 16 to 18 h and then heat shocked (a 42°C water bath for 30 min). At 6 h after the heat shock, the cells were washed with 1× PBS and lysed in 100 μl of NP-40 lysis buffer (50 mM Tris-HCl, pH 8.0, 150 mM NaCl, 1% NP-40) supplemented with a protease inhibitor cocktail tablet. The lysis procedure was carried out on ice for 10 min with occasional shaking. The lysate was centrifuged at 12,000 × *g* for 5 min, and an aliquot of the supernatant (10 μl) was reserved for Western blot analysis to confirm the expression of the transfected genes. The remaining supernatant (90 μl) was then incubated with 15 μl of anti-FLAG M2 affinity gel (Sigma) at 4°C overnight with rotation. The gel was then washed five times in 150 μl of NP-40 lysis buffer. Aliquots of the total cell lysates and immunoprecipitated complexes were separated by 15% SDS-PAGE and transferred to a polyvinylidene difluoride membrane. V5-tagged fusion proteins were detected with rabbit anti-V5 antibody and goat anti-rabbit IgG-HRP conjugate (Sigma). FLAG-tagged VP51A and VP26 proteins were detected with mouse anti-FLAG monoclonal antibody (Sigma) and goat anti-mouse IgG-HRP conjugate (Sigma).

Yeast two-hybrid assay. Protein-protein interaction assays were performed using a commercial yeast two-hybrid system, Matchmaker 3 (Clontech), according to the manufacturer's protocol. The bait plasmid, pGBK-VP51A, was constructed by cloning the PCR-amplified, full-length VP51A gene into the SmaI/BamHI sites of pGBKT7 (Clontech) in frame with the GAL4 DNA binding domain. The prey plasmids, pGAD-VP26 and pGAD-VP28, were constructed by cloning the PCR-amplified, full-length VP26 and VP28 genes, respectively, into the EcoRI/XhoI sites of pGADT7 (Clontech) in frame with the GAL4 activation domain. The PCR primer sequences are listed in Table 2. For the protein-protein interaction assay, *Saccharomyces cerevisiae* strain AH109 cells were cotransformed with the bait and prey plasmids using the lithium acetate method and plated on selective agar. The proteins were tested for autoactivation by cotransforming their respective plasmids with an empty prey or bait plasmid. For the positive control, the AH109 cells were cotransformed with plasmids pGBK-53 (p53) and pGAD-RecT (simian virus 40 large T antigen). Following transformation, the AH109 cells were plated onto synthetic defined (SD) medium lacking leucine (Leu) and tryptophan (Trp) to verify that both of the transformed plasmids were present. To select for yeast that contained interacting proteins, colonies that carried both plasmids were then plated onto SD medium lacking Leu, Trp, and histidine (His) and also onto SD medium lacking Leu, Trp, His,

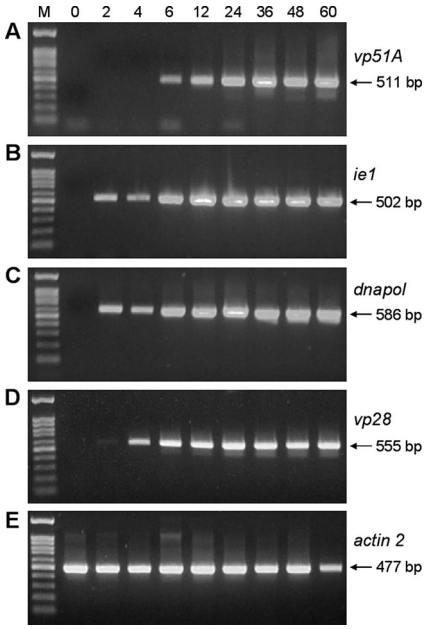

FIG. 1. Time course analysis of *vp51A* transcripts by RT-PCR. (A to E) Total RNAs were extracted from the gills of WSSV-infected shrimp and subjected to RT-PCR analysis with the indicated primers. Shrimp *actin 2* was included as a template control. The lane headings show times postinfection (hours). M, 100-bp DNA ladder. The arrows indicate the size of the amplicon for each gene.

and adenine (Ade) in the presence of 5-bromo-4-chloro-3-indolyl-α-D-galactopyranoside (X-α-Gal) (Sigma).

Indirect immunofluorescence assays of WSSV-infected shrimp hemocytes. Hemolymph was collected from healthy *P. monodon* shrimp and from WSSV-infected shrimp at 72 h p.i. using a syringe that contained cold modified Alsever solution (15). The hemocytes were placed on cover glasses, washed with PBS, and fixed in paraformaldehyde (4% in PBS) for 10 min at 4°C. After acetone treatment (3 min on ice), the hemocytes were incubated with blocking buffer (as described above) for 16 h at 4°C. The hemocytes were then treated with 500× PBS-diluted polyclonal rabbit anti-VP51A C-terminal antibody, 300× PBS-diluted polyclonal rat anti-VP26 antibody, or both (16 h at 4°C). Next, the cells were washed with PBST (three washes of 10 min each) and reacted with either 1,000× PBS-diluted Cy3 dye-conjugated donkey anti-rabbit IgG antibody, fluorescein isothiocyanate (FITC)-conjugated donkey anti-rat IgG antibody (1:500 in PBS; Jackson ImmunoResearch), or both for 2 h at room temperature. Counterstaining of the nucleus was performed with DAPI. After being washed three times with PBST (10 min each time), the cover glasses were wet mounted and the fluorescent signals were examined as described above.

RESULTS

Temporal-transcription analysis of *vp51A*. The expression profiles of *vp51A* in the gills of *P. monodon* at various stages of WSSV infection were analyzed by RT-PCR (Fig. 1). The *vp51A* transcript was first detected at 6 h p.i. By comparison, the immediate-early gene *ie1* and the early gene *dnapol* were both transcribed as early as 2 h p.i. and continued to be found to 60 h p.i. The transcript of the WSSV envelope protein gene *vp28* was also detected at 2 h p.i. The actin control confirmed the quantity of the total RNA templates (Fig. 1E), and another control using a WSSV genomic-DNA-specific primer pair, ICF2/IC-R3 (16), derived from an intergenic region of the WSSV genome, confirmed that there was no WSSV DNA contamination (data not shown). From these data, we conclude that *vp51A* is a gene that is expressed in the late stage of WSSV infection.

Mapping the 5′ and 3′ ends of the *vp51A* transcript by RACE. The 5′ and 3′ ends of the *vp51A* transcripts were determined by the RACE method. The 5′ RACE products were cloned into the pGEM-T Easy vector, and seven clones were randomly chosen for sequencing with the results shown in Fig. 2A. Two of the randomly selected 5′ RACE products had their 5′ termini at nucleotide residue −135 (G) and five at −128 (G) (relative to the A in the translation initiation codon, ATG, which is defined as +1 [A]) (Fig. 2A). These results suggest that for WSSV *vp51A*, there are two candidate transcription initiation sites, located at nucleotide residues −135 (G) and −128 (G), respectively. The sequence around −128 (G) did not match any of the known WSSV or baculovirus start site consensus motifs, and its biological meaning (if any) remains unclear. Conversely, the sequence around the transcriptional initiation site at −135 (G) (ATGAG) was a close match to the WSSV late-gene transcriptional initiation site consensus motif (ATNAC) (20). We also note that there was an A/T-rich region upstream of this site. In the 3′ region of *vp51A*, the polyadenylation signal (AATAAA) overlapped with the stop codon. Sequence analysis of the cloned 3′ RACE products revealed that the poly(A) tail addition site was located 22 bp downstream of the polyadenylation signal. Like many other WSSV genes (20), *vp51A* also had oligo(T) stretches downstream of the poly(A) tail addition site (Fig. 2B).

Localization of VP51A in the virion. In this study, we used a protein fractionation method developed by Tsai et al. (31) to determine whether VP51A is located in the envelope, the tegument, or the nucleocapsid. Using Western blot analysis of the eight different fractions of the WSSV virion proteins, VP51A's profile was compared to the profiles of known envelope, tegument, and nucleocapsid proteins (VP28, VP26, and VP51C, respectively) (Fig. 3). The results show that in the 1% Triton X-100-treated preparations, VP51A was similar to the envelope protein VP28 in that it was almost completely soluble in both the presence and absence of NaCl. The provisional conclusion that VP51A was therefore an envelope protein was then confirmed using an immunogold assay and IEM observation. When a gold-labeled secondary antibody was used in conjunction with an anti-VP51A antiserum derived from a C-terminal-region fragment (aa 251 to 486), gold particles were observed on the intact WSSV virions (Fig. 4A) but not on the tegument layer (Fig. 4B) or on the nucleocapsid surface (Fig. 4C). Control experiments showed that no gold particles were found on the envelopes of WSSV virions when normal rabbit serum was used as the primary antibody (Fig. 4D). Collectively, these results confirmed that VP51A is a WSSV envelope protein.

Molecular mass of the VP51A protein. Western blot analysis of the WSSV virion proteins using an antibody to a VP51A C-terminal fragment (aa 251 to 486) detected not only the theoretically predicted signal around 51 kDa, but also a major band at ~72 kDa (Fig. 5A). This unexpected result was checked using an antibody against the midsequence region (aa 139 to 250) of the VP51A coding region. The midsequence antibody detected the major band at ~72 kDa, as well as several other, smaller bands (Fig. 5B) that presumably resulted from posttranslational processing. The major 72-kDa band was

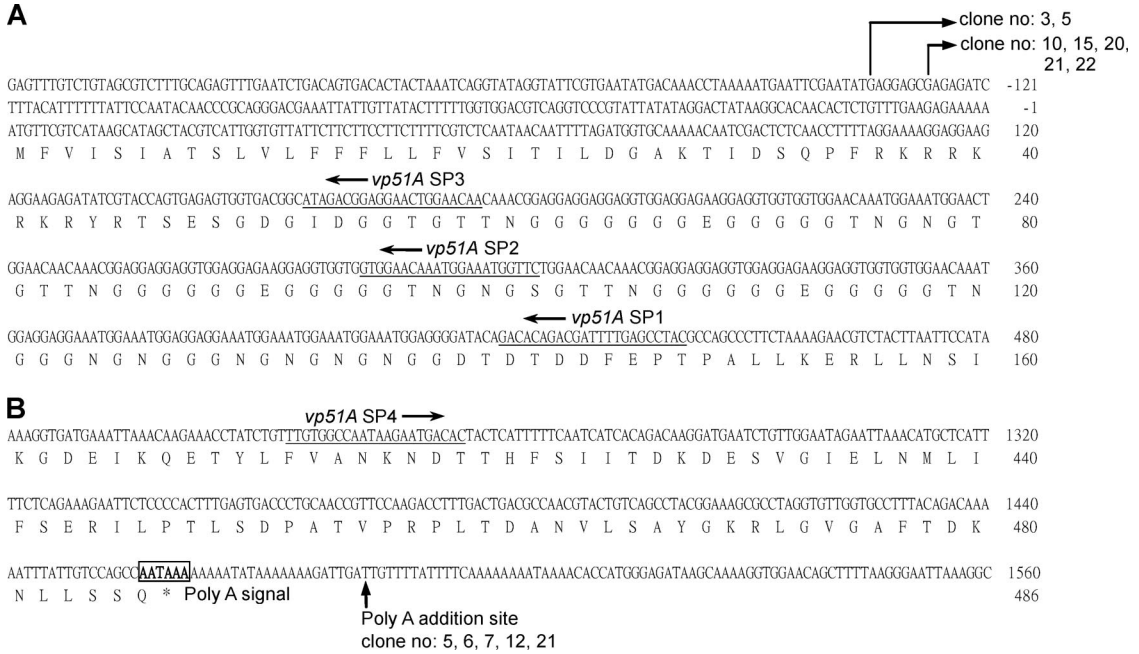

FIG. 2. Partial sequences of WSSV *vp51A* showing nucleotides and deduced amino acids for the 5′ (A) and 3′ (B) regions. The primers used for 5′ RACE and 3′ RACE (*vp51A* SP1, *vp51A* SP2, *vp51A* SP3, and *vp51A* SP4) are underlined. The bent arrows indicate the transcriptional start sites as revealed by sequencing seven randomly chosen 5′ RACE clones. The polyadenylation signal (AATAAA) is boxed and in boldface. The poly(A) addition site occurs 22 bp downstream of the polyadenylation signal and is indicated by a vertical arrow.

also detected using both V5 tagging (Fig. 5C, lane 2) and isotope labeling (Fig. 5D, lane 2). Figure 5E (lane 2) shows Western blots for a truncated form of *vp51A* (aa 51 to 486) that omitted the transmembrane domain in the N-terminal region and was expressed in *E. coli* cells. The molecular mass of this truncated, recombinant VP51A was about 68 kDa, which is a little lower than the molecular mass of the full-length VP51A that was overexpressed in Sf9 cells (Fig. 5E, compare lanes 2 and 3). Since no glycosylation can occur in the *E. coli* BL21 expression system, this result suggests that the 72-kDa band of VP51A was also not due to glycosylation. Although it is unusual for the structural proteins of animal viruses to remain unglycosylated, this finding for VP51A is consistent with previous reports that none of the WSSV structural proteins are glycosylated (35, 44). We therefore tentatively conclude that the discrepancy between the apparent molecular mass (72 kDa) and the calculated molecular mass (51.5 kDa) of VP51A must be due to the abundance of negatively charged residues (14%), which would have the effect of retarding the protein's migration through the gel (4, 7).

Membrane topology of VP51A. A hydrophobicity profile generated using Kyte-Doolittle hydropathy plot analysis showed a

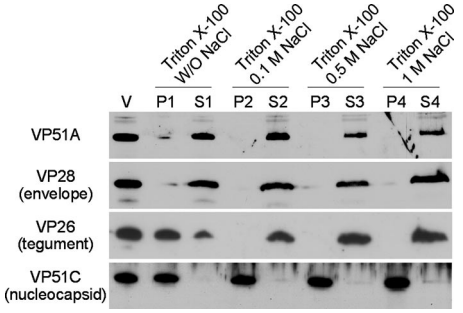

FIG. 3. Determination of VP51A's location in the WSSV virion. Intact WSSV virions were subjected to detergent and NaCl treatment as indicated. After fractionation, the pellet (P) and supernatant (S) fractions were separated on SDS-PAGE and detected by Western blotting to produce profiles that are characteristic of envelope, tegument, and nucleocapsid proteins (31). Three representative WSSV structural proteins are shown for comparison. Lane V is the untreated purified virus.

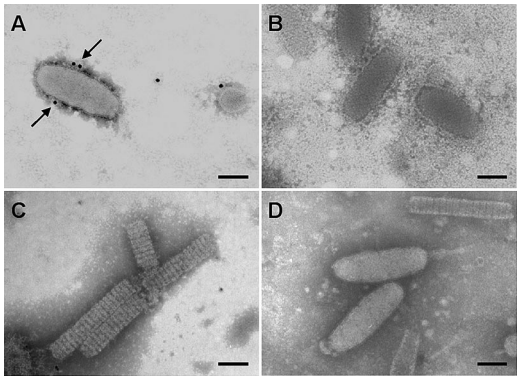

FIG. 4. Localization of VP51A in the WSSV virion by immunogold assay using a rabbit anti-VP51A C-terminal antibody probe followed by a gold-labeled secondary antibody. (A to C) IEM images of purified WSSV virions (A), unenveloped virions (i.e., the tegument-nucleocapsid structure) (B), and the viral nucleocapsids (C). (D) IEM of WSSV virions, with preimmune rabbit serum used as the probe instead of the primary antibodies. The gold particle signals (arrows) were detected only on the enveloped virion. Scale bars, 100 nm.

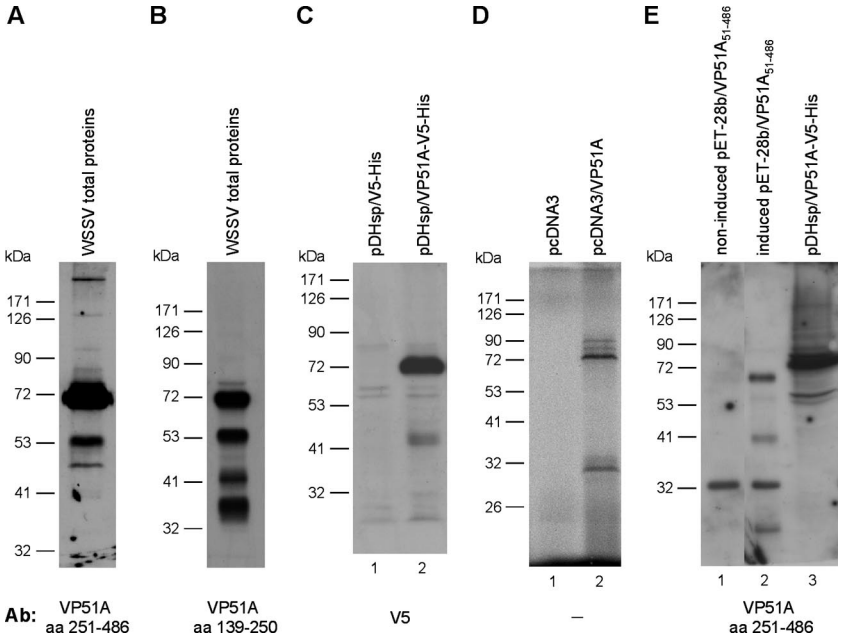

FIG. 5. Molecular masses of the VP51A protein. (A and B) Total proteins from WSSV virions were probed with antibodies to either the C-terminal (aa 251 to 486) (A) or midsequence (aa 139 to 250) (B) region of VP51A. (C) Western blotting using anti-V5 antibody to detect transiently expressed V5-tagged VP51A in Sf9 cells (lane 2). Lane 1 is the empty vector. (D) Coupled in vitro transcription and translation products of the empty vector (lane 1) and plasmids containing the VP51A gene (lane 2). (E) Total proteins of IPTG-induced (lane 2) and noninduced (lane 1) pET-28b/VP51A$_{51-486}$-transformed *E. coli* BL21 and pDHsp/VP51A-V5-His-transfected Sf9 cells (lane 3) probed with anti-VP51A C-terminal antibody.

high hydrophobicity in the N-terminal region of VP51A (data not shown), while sequence analysis of VP51A using the TMHMM program predicted that VP51A encodes a transmembrane helix between aa 2 and 24 (data not shown). To confirm these predictions, a recombinant VP51A fusion protein (rVP51A-V5) with a V5 tag on its C terminus was subjected to indirect immunofluorescence assays in transfected Sf9 cells. In cells that were treated with Triton X-100 to render them permeable to the anti-V5 antibody, the full-length rVP51A-V5 was detected both in the plasma membrane region and in the cytoplasm (Fig. 6A, top). In the nonpermeabilized cells, however, even though the rVP51A-V5 could no longer be detected in the cytoplasm, it was still detected on the outside surface of the plasma membrane (Fig. 6A, bottom). We conclude that the C-terminal region of the protein must therefore be located outside the cell membrane, because otherwise the V5 tag would not have been accessible to the anti-V5 antibody. This conclusion was further confirmed by conducting a similar assay for PmSTAT, a shrimp protein that is expressed in both the nucleus and cytoplasm of Sf9 cells (17). We found that in the absence of Triton X-100, no positive PmSTAT signals could be detected (data not shown). Taken together, these data suggest that VP51A is a type II transmembrane protein. A schematic of the proposed transmembrane topology of the V5-tagged VP51A is shown in Fig. 6B.

Virion topology of VP51A, VP26, and VP28. The topology of these three structural proteins in the WSSV virion was investigated by using trypsin to distinguish between proteins that were accessible to proteolysis and those that were protected from digestion by the lipid bilayer. WSSV virions were either left untreated or treated with trypsin in the absence or pres-

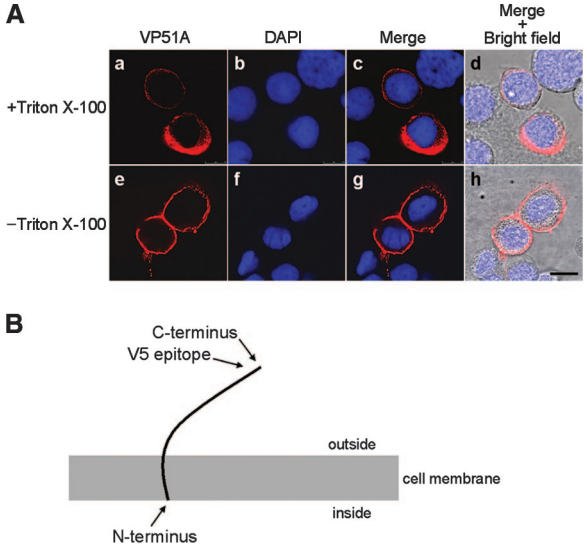

FIG. 6. Membrane topology of WSSV VP51A. (A) V5-tagged recombinant VP51A was transiently expressed in Sf9 cells that were fixed with paraformaldehyde and permeabilized with Triton X-100 (a to d) or not permeabilized (e to h). rVP51A-V5 was visualized with rabbit anti-V5 antibody and Cy3-conjugated donkey anti-rabbit IgG antibody (a and e). Nuclei were visualized by counterstaining them with DAPI (b and f). Images c and g show the merged Cy3 and DAPI signals. The last column (d and h) shows the merged signal overlaid with the bright-field images of the corresponding cells. Scale bar, 10 μm. (B) Schematic of the proposed transmembrane topology of VP51A.

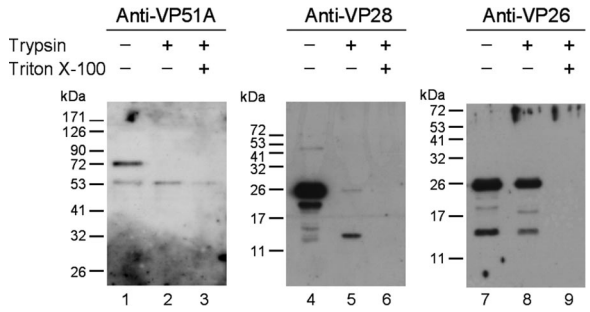

FIG. 7. Western blot analysis showing trypsin digestion of VP51A and two representative proteins, VP28 (envelope) and VP26 (tegument), in intact and detergent-treated virions. VP51A was detected using the antibody to its C terminus (aa 251 to 486).

ence of the detergent Triton X-100, and the digested products were analyzed by Western immunoblotting using antibodies against the VP51A C terminus (aa 251 to 486) or against the full length of VP26 or VP28. As expected, the VP51A antibody recognized the VP51A 72- and 51-kDa proteins in the untreated virions (Fig. 7, lane 1). However, after digestion with trypsin in the absence or presence of Triton X-100, the 72-kDa protein was no longer detected, even though the 51-kDa protein was still present (Fig. 7, lanes 2 and 3). We note that the amount of the 51-kDa protein was only slightly decreased in the presence of Triton X-100 (Fig. 7, lane 3), which suggests that the 51-kDa VP51A protein was still protected from trypsin digestion even after the envelope was removed. Similar immunoblotting results were obtained with the antibody against the VP51A midsequence (data not shown). It is not clear why the 51-kDa VP51A was not degraded by trypsin digestion. The treated virions were also subjected to Western blotting to detect the envelope protein VP28 and the tegument protein VP26. VP28 was digested into two bands in the absence of Triton X-100 and completely digested in the presence of Triton X-100 (Fig. 7, lanes 4 to 6). VP26 was digested only in the presence of Triton X-100 (Fig. 7, lanes 7 to 9). Similar results for VP26 and VP28 were also demonstrated by Tsai et al. (31).

VP51A interacts with VP26. Interactions between VP51A and two major WSSV structural proteins, VP26 and VP28, were investigated using a coimmunoprecipitation assay in which FLAG-tagged VP51A (VP51A-FLAG)/V5-tagged VP26 (VP26-V5), or VP51A-FLAG/V5-tagged VP28 (VP28-V5) was coexpressed in Sf9 insect cells. As shown in Fig. 8A, a, all three of these inputs, VP26-V5, VP28-V5, and VP51A-FLAG, were successfully expressed in the Sf9 cells, and a pilot experiment confirmed that the VP51A-FLAG proteins could be efficiently precipitated by the anti-FLAG antibody (data not shown). In the coimmunoprecipitation assays, VP26-V5 was coimmunoprecipitated with VP51A-FLAG while VP28-V5 was not (Fig. 8A, b, lanes 3 and 5). A reverse experiment using FLAG-tagged VP26 and V5-tagged VP51A produced the same results (data not shown). The binding specificity of VP51A-FLAG with anti-FLAG M2 affinity gel was reconfirmed by subjecting VP51A-FLAG protein to reaction with anti-hemagglutinin antibody-conjugated beads (data not shown). From these results, we conclude that the interaction between VP51A and VP26 is specific and independent of the tags. The interaction between VP51A and VP26 was further confirmed

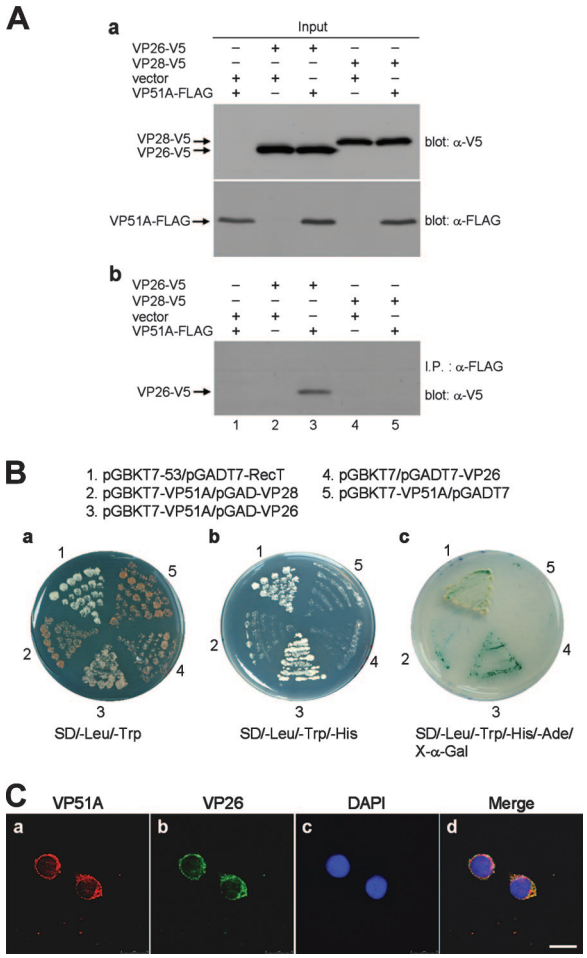

FIG. 8. VP51A interacts with VP26, but not with VP28. (A) Coimmunoprecipitation of V5-tagged VP26 or VP28 with FLAG-tagged VP51A from transfected cells. Sf9 cells were transfected with plasmids expressing V5-tagged VP26, V5-tagged VP28, FLAG-tagged VP51A, or empty plasmid (vector) as indicated. (a) At 6 h after heat shock, the cell lysates were harvested and separated by SDS-PAGE, and input expression was confirmed by Western blotting (blot) using either anti-V5 antibody or anti-FLAG antibody as a probe. The arrows indicate the expressed V5-tagged VP26, V5-tagged VP28, and FLAG-tagged VP51A. (b) The cell lysates were immunoprecipitated (I.P.) with anti-FLAG M2 affinity resins, and then the immunoprecipitated complexes were subjected to Western blot analysis with an anti-V5 antibody probe. (B) The yeast two-hybrid results confirmed that VP51A specifically interacted with VP26, but not with VP28. (a) Yeast growth on medium lacking both Leu and Trp indicated the presence of each respective pair of plasmids. (b and c) Yeast growth on low-stringency (−Leu/−Trp/−His) and high-stringency (−Leu/−Trp/−His/−Ade) media, respectively. The blue signal in image c is due to the presence of X-α-Gal. The positive signals represent protein-protein interactions. (C) Intracellular localizations of VP51A and VP26 in WSSV-infected *P. monodon* hemocytes by confocal microscopy. (a) VP51A was visualized using rabbit anti-VP51A antibody and Cy3-conjugated donkey anti-rabbit IgG antibody. (b) VP26 was visualized with rat anti-VP26 antibody and FITC-conjugated donkey anti-rat IgG antibody. (c) Nuclei were visualized by counterstaining them with DAPI. (d) Merged Cy3, FITC, and DAPI signals. Scale bar, 10 μm.

by a yeast two-hybrid assay. Image a in Fig. 8B shows that all of the cotransformants were able to grow on the SD/−Leu/−Trp plate, and all of these constructs were also able to be expressed successfully in yeast cells (data not shown). The

VP51A protein and the empty vector (pGBK-VP51A/pGADT7) did not induce reporter gene activation (Fig. 8B, b and c), from which we conclude that VP51A does not have autonomous activation ability. Growth on the low-stringency (SD/−Leu/−Trp/−His) and high-stringency (SD/−Leu/−Trp/−His/−Ade/X-α-Gal) plates was observed only when the yeast was transformed with pGBK-VP51A/pGAD-VP26 or with the positive control (Fig. 8B, b and c). Again, these results showed that VP51A interacts with VP26 but does not interact with VP28.

In order to assess the intracellular distribution of VP51A and VP26 in WSSV-infected *P. monodon* cells, hemocytes were collected at a late stage of infection (72 h p.i.). The virus-infected cells were fixed, permeabilized, stained for rabbit anti-VP51A and rat anti-VP26 antibodies, and analyzed by confocal microscopy. As shown in Fig. 8C, strong punctate signals from both VP51A (image a) and from VP26 (image b) were observed in the plasma membrane and cytoplasm, and the merged image shows that these signals were almost completely superimposed (image d). No signals were detected in the uninfected *P. monodon* hemocyte controls (data not shown). Clearly, this suggests that both VP51A and VP26 colocalized to the same subcellular locations.

VP26 links VP51A and VP28. A previous study showed that VP26 interacts with the most abundant envelope protein, VP28 (44), and this result was reconfirmed here by a coimmunoprecipitation assay with V5-tagged VP28 and FLAG-tagged VP26 expressed in Sf9 insect cells. The two images in Fig. 9A, a, show that both VP26-FLAG and VP28-V5 were successfully expressed in Sf9 cells. Complexes consisting of VP28-V5 plus VP26-FLAG were coimmunoprecipitated by anti-FLAG M2 affinity gel and detected by Western blotting with anti-V5 antibody (Fig. 9A, b, lane 2). As discussed above, we had already established that VP51A interacts with VP26 but not with VP28 (Fig. 8A and B), so we next designed a coimmunoprecipitation experiment to investigate the interactions among all three of these proteins. Expression of VP51A-FLAG, VP26-V5, and VP28-V5 in the cotransfected Sf9 cells was confirmed by Western blot analysis with anti-FLAG and anti-V5 antibodies (Fig. 9B, a). The putative VP51A-VP26-VP28 complex was immunoprecipitated by using an anti-FLAG M2 affinity gel against the FLAG epitope on VP51A, and the presence of both VP26 and VP28 in the complex was demonstrated by Western blotting using anti-V5 antibody (Fig. 9B, b). For the control, cells were cotransfected with an empty V5 vector instead of the VP26-V5 plasmid, with the result that neither VP26 nor VP28 was observed in the Western blot analysis (Fig. 9B, b, lane 1). We therefore conclude that VP26 plays a key role in the formation of a VP51A-VP26-VP28 ternary complex.

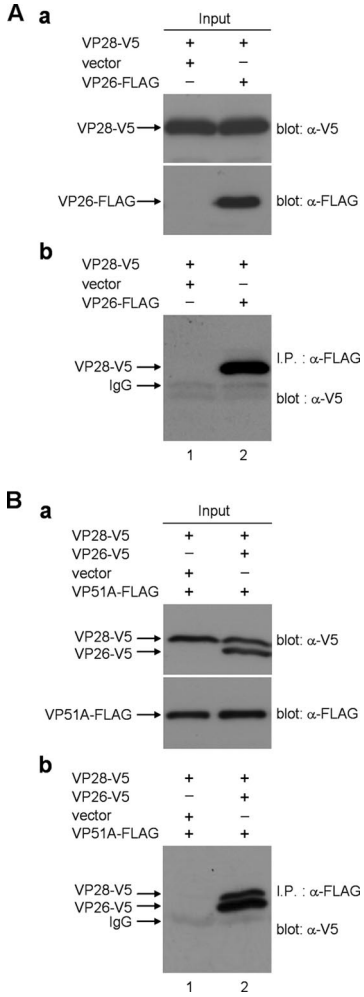

FIG. 9. VP51A, VP26, and VP28 form a ternary complex. (A) (a) V5-tagged VP28 was transiently coexpressed in Sf9 cells with either the empty plasmid (vector) or a plasmid that expressed FLAG-tagged VP26. At 6 h after heat shock, the cell lysates were harvested and input expression was monitored using Western blot (blot) analysis with either anti-V5 or anti-FLAG antibody as the probe. (b) Lysates from cells cotransfected with V5-tagged VP28 and vector or with V5-tagged VP28 and FLAG-tagged VP26 were immunoprecipitated (I.P.) with anti-FLAG M2 affinity resins. The immunoprecipitated complexes were then subjected to Western blot analysis with an anti-V5 antibody probe. Bands corresponding to the V5-tagged VP28 and nonspecific bound IgG are indicated. (B) (a) Sf9 cells were cotransfected with plasmids expressing FLAG-tagged VP51A, V5-tagged VP28, and V5-tagged VP26. For the control, the VP26 plasmid was replaced by empty plasmid (vector). Expression of each input was confirmed by Western blot analysis of the cell lysates with the indicated antibodies. (b) At 6 h after heat shock, the cell lysates were harvested and immunoprecipitated with anti-FLAG M2 affinity resins. The immunoprecipitates were then subjected to Western blot analysis with an anti-V5 antibody probe, and both V5-tagged VP26 and VP28 and the nonspecific bound IgG were detected.

DISCUSSION

Our results suggest that the major VP51A protein species is unglycosylated and that its apparent mass of 72 kDa is in fact due to a high proportion of charged residues that retard the protein's migration in the gel. We note that two earlier studies identified only a single VP51A (or VP52A) band in the region of ~51 kDa, and neither study reported the major 72-kDa band. In one study (32), the 72-kDa region of the gel was dominated by a very high-intensity band of crayfish hemocyanin that obscured all of the neighboring bands. In the other study (44), the 72-kDa VP51A protein was not reported, even though the entire crayfish was used as the source material and the problem of hemocyanin contamination was solved by using a different purification method. We found, however, that by using the same source tissues and protocols as Xie et al. (44),

we were able to detect the 72-kDa VP51A in the purified virions, and in fact, Western blotting showed that the smaller species of VP51A (i.e., 51 kDa and others) (Fig. 5A and B) were consistently present as well (data not shown). Since the 51-kDa protein could be detected by both the anti-VP51A midsequence and C-terminal antibodies (Fig. 5A and B) and since the peptide sequences deduced from the tandem mass spectrometry data of Tsai et al. (32) matched only the C-terminal region of VP51A (J.-M. Tsai, personal communication), we hypothesize that the 51-kDa band was in fact produced by N-terminal truncation of the full-length protein. Further, since Western blotting consistently produced the same protein profiles regardless of the purification method that was used, we infer that VP51A is sensitive only to site-specific proteases and is otherwise not easily degraded. Lastly, we note that since the 72-kDa, 51-kDa, and some other, smaller VP51A proteins are all readily detected in the WSSV virion (Fig. 5A and B), it seems likely that all of these forms are essential components of the viral particle, and they may all participate at various stages of virus morphogenesis.

We note that there is similar evidence for the proteolytic processing of at least one other WSSV structural protein. Xie et al. (44) identified five different species of VP150 in purified WSSV virions, and the smallest of these proteins had the same apparent mass as VP53A of Tsai et al. (32). Since these two studies used different purification methods, and since VP53A and the 53-kDa species of VP150 were both identified as products of the same open reading frame (WSV011 in the China isolate; WSSV067 in the Taiwan isolate), we hypothesize that WSSV VP150 may also be subjected to proteolytic processing by a specific virus or host protease.

The ability of WSSV to replicate successfully in a wide range of crustacean hosts suggests that a common crustacean protease might be involved in VP51A proteolysis. Furin is one possible candidate. This extensively studied cellular proprotein convertase is used by many cleavable viral envelope proteins (23, 28), and in WSSV VP51A, we found two overlapping instances of the furin recognition motif RXK/RR near the N terminus (^{36}RKRRKR^{41}). However, our pilot experiments suggested that furin is not in fact involved in the proteolytic processing of the VP51A 72-kDa protein molecule (data not shown). Thus, for the moment, the cellular or viral factors involved in VP51A cleavage and the events governing the trafficking of the precursors remain unknown.

The protein domains exposed on the surfaces of viruses play fundamental roles in infection by binding to cell receptors, promoting cell fusion processes, or interacting with elements of the host immune system (1, 24, 26). Thus, the determination of a protein's membrane topology is an important first step toward understanding its function. Topological predictions made by the program TMHMM suggested that VP51A encodes a transmembrane helix near its N terminus and that the entire C-terminal region of the protein is on the outside surface of the plasma membrane. Other membrane topology and hydropathic prediction programs yielded similar results (data not shown). Immunofluorescence assays performed on recombinant VP51A fusion protein expressed in Sf9 cells confirmed these predictions; that is, in the intact Sf9 cells, the C-terminal V5 epitopes of the recombinant VP51A could be detected only on the outer surfaces of the cell membranes (Fig. 6A). In the WSSV virions, VP51A topology was investigated using two experimental approaches. First, an antibody to the VP51A C terminus directly recognized VP51A on the outer surfaces of the envelopes of purified intact virions (Fig. 4A), and second, trypsin digestion of the VP51A 72-kDa protein in the absence of detergent (Fig. 7, lane 2) also confirmed that the C terminus of VP51A was exposed on the outside of the virion.

Interactions between structural proteins are common in enveloped viruses, but to date, protein-protein interactions have been reported only in four major WSSV virion proteins, VP24, VP26, VP28, and WSV010 (3, 43, 44). In the present study, we found that VP51A formed a ternary complex with VP26 and VP28, with VP26 acting as the linker protein (Fig. 8 and 9). The functional significance of this complex is unknown, but we note that VP26 and VP28 are both major WSSV structural proteins. VP28 is an envelope protein that is implicated in cell attachment during infection (12, 34, 46), and although the location of VP26 is still disputed (e.g., by Tang et al. [30]), most of the recent evidence (31, 42, 44) (Fig. 7) suggests that it is in fact a tegument or linker protein. In the virion, the hydrophobic N-terminal region of VP26 may be anchored in the envelope, while its C terminus is bound to the nucleocapsid (42). Based on the fact that VP26 binds with actin, Xie and Yang (42) further hypothesized that it may be instrumental in trafficking the WSSV nucleocapsid into the host nucleus via the cytoskeleton. Given the propensity of VP51A to form a complex with VP26 and VP28, it will be interesting to investigate the extent to which VP51A may contribute to the functionality of either or both of these two major WSSV structural proteins.

ACKNOWLEDGMENTS

This investigation was supported financially by National Science Council grants (NSC95-2313-B-212-006-MY2, NSC96-2317-B-002-015, and NSC96-2317-B-002-020).

We are indebted to Paul Barlow for his helpful criticism.

REFERENCES

1. **Campadelli-Fiume, G., M. Amasio, E. Avitabile, A. Cerretani, C. Forghieri, T. Gianni, and L. Menotti.** 2007. The multipartite system that mediates entry of herpes simplex virus into the cell. Rev. Med. Virol. **17:**313–326.
2. **Chazal, N., and D. Gerlier.** 2003. Virus entry, assembly, budding, and membrane rafts. Microbiol. Mol. Biol. Rev. **67:**226–237.
3. **Chen, J., Z. Li, and C.-L. Hew.** 2007. Characterization of a novel envelope protein WSV010 of shrimp white spot syndrome virus and its interaction with a major viral structural protein VP24. Virology **364:**208–213.
4. **Dunker, A. K., and R. R. Rueckert.** 1969. Observations on molecular weight determinations on polyacrylamide gel. J. Biol. Chem. **244:**5074–5080.
5. **Escobedo-Bonilla, C. M., V. Alday-Sanz, M. Wille, P. Sorgeloos, M. B. Pensaert, and H. J. Nauwynck.** 2008. A review on the morphology, molecular characterization, morphogenesis and pathogenesis of white spot syndrome virus. J. Fish Dis. **31:**1–18.
6. **Frohman, M. A., M. K. Dush, and G. R. Martin.** 1988. Rapid production of full-length cDNAs from rare transcripts: amplification using a single gene-specific oligonucleotide primer. Proc. Natl. Acad. Sci. USA **85:**8998–9002.
7. **Graceffa, P., A. Jancso, and K. Mabuchi.** 1992. Modification of acidic residues normalizes sodium dodecyl sulfate-polyacrylamide gel electrophoresis of caldesmon and other proteins that migrate anomalously. Arch. Biochem. Biophys. **297:**46–51.
8. **Kim, C. S., Z. Kosuke, Y. K. Nam, S. K. Kim, and K. H. Kim.** 2007. Protection of shrimp (*Penaeus chinensis*) against white spot syndrome virus (WSSV) challenge by double-stranded RNA. Fish Shellfish Immunol. **23:** 242–246.
9. **Krogh, A., B. Larsson, G. von Heijne, and E. L. Sonnhammer.** 2001. Predicting transmembrane protein topology with a hidden Markov model: application to complete genomes. J. Mol. Biol. **305:**567–580.
10. **Kyte, J., and R. F. Doolittle.** 1982. A simple method for displaying the hydropathic character of a protein. J. Mol. Biol. **157:**105–132.
11. **Leu, J.-H., Y.-C. Kuo, G.-H. Kou, and C.-F. Lo.** 2008. Molecular cloning and characterization of an inhibitor of apoptosis protein (IAP) from the tiger shrimp, *Penaeus monodon*. Dev. Comp. Immunol. **32:**121–133.

12. **Li, L. J., J. F. Yuan, C. A. Cai, W. G. Gu, and Z. L. Shi.** 2006. Multiple envelope proteins are involved in white spot syndrome virus (WSSV) infection in crayfish. Arch. Virol. **151:**1309–1317.
13. **Li, Z., Q. Lin, J. Chen, J. L. Wu, T. K. Lim, S. S. Loh, X. Tang, and C.-L. Hew.** 2007. Shotgun identification of the structural proteome of shrimp white spot syndrome virus and iTRAQ differentiation of envelope and nucleocapsid subproteomes. Mol. Cell Proteomics. **6:**1609–1620.
14. **Liang, Y., J. Huang, X.-L. Song, P.-J. Zhang, and H.-S. Xu.** 2005. Four viral proteins of white spot syndrome virus (WSSV) that attach to shrimp cell membranes. Dis. Aquat. Organ. **66:**81–85.
15. **Lin, S.-T., Y.-S. Chang, H.-C. Wang, H.-F. Tzeng, T.-Z. Chang, J.-Y. Lin, C.-H. Wang, C.-F. Lo, and G.-H. Kou.** 2002. Ribonucleotide reductase of shrimp white spot syndrome virus (WSSV): expression and enzymatic activity in a baculovirus/insect cell system and WSSV-infected shrimp. Virology **304:**282–290.
16. **Liu, W.-J., H.-T. Yu, S.-E. Peng, Y.-S. Chang, H.-W. Pien, C.-J. Lin, C.-J. Huang, M.-F. Tsai, C.-J. Huang, C.-H. Wang, J.-Y. Lin, C.-F. Lo, and G.-H. Kou.** 2001. Cloning, characterization and phylogenetic analysis of a shrimp white spot syndrome virus (WSSV) gene that encodes a protein kinase. Virology **289:**362–377.
17. **Liu, W.-J., Y.-S. Chang, A. H.-J. Wang, G.-H. Kou, and C.-F. Lo.** 2007. White spot syndrome virus annexes a shrimp STAT to enhance expression of the immediate-early gene *ie1*. J. Virol. **81:**1461–1471.
18. **Lo, C.-F., H.-C. Hsu, M.-F. Tsai, C.-H. Ho, S.-E. Peng, G.-H. Kou, and D. V. Lightner.** 1999. Specific genomic DNA fragments analysis of different geographical clinical samples of shrimp white spot syndrome virus. Dis. Aquat. Organ. **35:**175–185.
19. **Lo, C.-F., S.-E. Peng, Y.-S. Chang, and G.-H. Kou.** 2005. White spot syndrome—what we have learned about the virus and the disease, p. 421–433. *In* P. J. Walker, R. G. Lester, and M. G. Bondad-Reantaso (ed.), Diseases in Asian aquaculture V. Proceedings of the 5th Symposium on Diseases in Asian Aquaculture. Fish Health Section, Asian Fisheries Society, Manila, Philippines.
20. **Marks, H., X.-Y. Ren, H. Sandbrink, M. C. W. van Hulten, and J. M. Vlak.** 2006. *In silico* identification of putative promoter motifs of white spot syndrome virus. BMC Bioinformatics **7:**309. http://www.biomedcentral.com/1471–2105/7/309.
21. **Mettenleiter, T. C.** 2004. Budding events in herpesvirus morphogenesis. Virus Res. **106:**167–180.
22. **Mettenleiter, T. C., B. G. Klupp, and H. Granzow.** 2006. Herpesvirus assembly: a tale of two membranes. Curr. Opin. Microbiol. **9:**423–429.
23. **Nakayama, K.** 1997. Furin: a mammalian subtilisin/Kex2p-like endoprotease involved in processing of a wide variety of precursor proteins. Biochem. J. **327:**625–635.
24. **Rajcáni, J.** 2003. Molecular mechanisms of virus spread and virion components as tools of virulence. A review. Acta Microbiol. Immunol. Hung. **50:**407–431.
25. **Rajesh Kumar, S., V. P. Ishaq Ahamed, M. Sarathi, A. Nazeer Basha, and A. S. Sahul Hameed.** 2008. Immunological responses of *Penaeus monodon* to DNA vaccine and its efficacy to protect shrimp against white spot syndrome virus (WSSV). Fish Shellfish Immunol. **24:**467–478.
26. **Reske, A., G. Pollara, C. Krummenacher, B. M. Chain, and D. R. Katz.** 2007. Understanding HSV-1 entry glycoproteins. Rev. Med. Virol. **17:**205–215.
27. **Robalino, J., T. Bartlett, E. Shepard, S. Prior, G. Jaramillo, E. Scura, R. W. Chapman, P. S. Gross, C. L. Browdy, and G. W. Warr.** 2005. Double-stranded RNA induces sequence-specific antiviral silencing in addition to nonspecific immunity in a marine shrimp: convergence of RNA interference and innate immunity in the invertebrate antiviral response? J. Virol. **79:**13561–13571.
28. **Rockwell, N. C., and J. W. Thorner.** 2004. The kindest cuts of all: crystal structures of Kex2 and furin reveal secrets of precursor processing. Trends Biochem. Sci. **29:**80–87.
29. **Rout, N., S. Kumar, S. Jaganmohan, and V. Murugan.** 2007. DNA vaccines encoding viral envelope proteins confer protective immunity against WSSV in black tiger shrimp. Vaccine **25:**2778–2786.
30. **Tang, X., J. Wu, J. Sivaraman, and C.-L. Hew.** 2007. Crystal structures of major envelope proteins VP26 and VP28 from white spot syndrome virus shed light on their evolutionary relationship. J. Virol. **81:**6709–6717.
31. **Tsai, J.-M., H.-C. Wang, J.-H. Leu, A. H.-J. Wang, Y. Zhuang, P. J. Walker, G.-H. Kou, and C.-F. Lo.** 2006. Identification of the nucleocapsid, tegument, and envelope proteins of the shrimp white spot syndrome virus virion. J. Virol. **80:**3021–3029.
32. **Tsai, J.-M., H.-C. Wang, J.-H. Leu, H.-H. Hsiao, A. H.-J. Wang, G.-H. Kou, and C.-F. Lo.** 2004. Genomic and proteomic analysis of thirty-nine structural proteins of shrimp white spot syndrome virus. J. Virol. **78:**11360–11370.
33. **Tsai, M.-F., G.-H. Kou, H.-C. Liu, K.-F. Liu, C.-F. Chang, S.-E. Peng, H.-C. Hsu, C.-H. Wang, and C.-F. Lo.** 1999. Long-term presence of white spot syndrome virus (WSSV) in a cultured shrimp population without disease outbreaks. Dis. Aquat. Organ. **38:**107–114.
34. **van Hulten, M. C. W., J. Witteveldt, M. Snippe, and J. M. Vlak.** 2001. White spot syndrome virus envelope protein VP28 is involved in the systemic infection of shrimp. Virology **285:**228–233.
35. **van Hulten, M. C. W., M. Reijns, A. M. G. Vermeesch, F. Zandbergen, and J. M. Vlak.** 2002. Identification of VP19 and VP15 of white spot syndrome virus (WSSV) and glycosylation status of the WSSV major structural proteins. J. Gen. Virol. **83:**257–265.
36. **Vaseeharan, B., T. Prem Anand, T. Murugan, and J. C. Chen.** 2006. Shrimp vaccination trials with the VP292 protein of white spot syndrome virus. Lett. Appl. Microbiol. **43:**137–142.
37. **Vlak, J. M., J. R. Bonami, T. W. Flegel, G.-H. Kou, D. V. Lightner, C.-F. Lo, P. C. Loh, and P. J. Walker.** 2004. *Nimaviridae*, p. 187–192. *In* C. M. Fauquet, M. A. Mayo, J. Maniloff, U. Desselberger, and L. A. Ball (ed.), Virus taxonomy. Eighth report of the International Committee on Taxonomy of Viruses. Elsevier Academic Press, San Diego, CA.
38. **Wang, C.-H., C.-F. Lo, J.-H. Leu, C.-M. Chou, P.-Y. Yeh, H.-Y. Chou, M.-C. Tung, C.-F. Chang, M.-S. Su, and G.-H. Kou.** 1995. Purification and genomic analysis of baculovirus associated with white spot syndrome (WSBV) of *Penaeus monodon*. Dis. Aquat. Organ. **23:**239–242.
39. **Witteveldt, J., J. M. Vlak, and M. C. W. van Hulten.** 2004. Protection of *Penaeus monodon* against white spot syndrome virus using a WSSV subunit vaccine. Fish Shellfish Immunol. **16:**571–579.
40. **Wu, C., and F. Yang.** 2006. Localization studies of two white spot syndrome virus structural proteins VP51 and VP76. Virol. J. **3:**76. http://www.virologyj.com/content/3/1/76.
41. **Wu, W., L. Wang, and X. Zhang.** 2005. Identification of white spot syndrome virus (WSSV) envelope proteins involved in shrimp infection. Virology **332:**578–583.
42. **Xie, X., and F. Yang.** 2005. Interaction of white spot syndrome virus VP26 protein with actin. Virology **336:**93–99.
43. **Xie, X., and F. Yang.** 2006. White spot syndrome virus VP24 interacts with VP28 and is involved in virus infection. J. Gen. Virol. **87:**1903–1908.
44. **Xie, X., L. Xu, and F. Yang.** 2006. Proteomic analysis of the major envelope and nucleocapsid proteins of white spot syndrome virus. J. Virol. **80:**10615–10623.
45. **Xu, J., F. Han, and X. Zhang.** 2007. Silencing shrimp white spot syndrome virus (WSSV) genes by siRNA. Antivir. Res. **73:**126–131.
46. **Yi, G., Z. Wang, Y. Qi, L. Yao, J. Qian, and L. Hu.** 2004. VP28 of white spot syndrome virus is involved in the attachment and penetration into shrimp cells. J. Biochem. Mol. Biol. **37:**726–734.
47. **Zhang, X., C. Huang, X. Tang, Y. Zhuang, and C.-L. Hew.** 2004. Identification of structural proteins from shrimp white spot syndrome virus (WSSV) by 2DE-MS. Proteins **55:**229–235.
48. **Zhu, F. X., and Y. Yuan.** 2003. The ORF45 protein of Kaposi's sarcoma-associated herpesvirus is associated with purified virions. J. Virol. **77:**4221–4230.